Published in final edited form as:
Respir Physiol Neurobiol. 2013 August 15; 188(2): 83–93. doi:10.1016/j.resp.2013.05.013.

Bicarbonate-sensitive soluble and transmembrane adenylyl cyclases in peripheral chemoreceptors

Ana R. Nunes[a,b], **Andrew P.S. Holmes**[c], **Vedangi Sample**[d], **Prem Kumar**[c], **Martin J. Cann**[e], **Emília C. Monteiro**[b], **Jin Zhang**[d], and **Estelle B. Gauda**[a,*]

[a]Department of Pediatrics, Johns Hopkins Medical Institutions, Baltimore, MD, USA

[b]CEDOC, Farmacologia, Faculdade de Ciências Médicas, FCM, Universidade Nova de Lisboa, Portugal

[c]School of Clinical and Experimental Medicine, College of Medical and Dental Sciences, University of Birmingham, Birmingham, UK

[d]Department of Pharmacology and Molecular Sciences, Johns Hopkins Medical Institutions, Baltimore, MD, USA

[e]School of Biological and Biomedical Sciences, Durham University, UK

Abstract

Stimulation of the carotid body (CB) chemoreceptors by hypercapnia triggers a reflex ventilatory response via a cascade of cellular events, which includes generation of cAMP. However, it is not known if molecular CO_2/HCO_3^- and/or H^+ mediate this effect and how these molecules contribute to cAMP production. We previously reported that the CB highly expresses HCO_3^--sensitive soluble adenylyl cyclase (sAC). In the present study we systematically characterize the role of sAC in the CB, comparing the effect of isohydric hypercapnia (IH) in cAMP generation through activation of sAC or transmembrane-adenylyl cyclase (tmAC).

Pharmacological deactivation of sAC and tmAC decreased the CB cAMP content in normocapnia and IH with no differences between these two conditions. Changes from normocapnia to IH did not effect the degree of PKA activation and the carotid sinus nerve discharge frequency.

sAC and tmAC are functional in CB but intracellular elevations in CO_2/HCO_3^- in IH conditions on their own are insufficient to further activate these enzymes, suggesting that the hypercapnic response is dependent on secondary acidosis.

Keywords

Carotid body; cAMP; Adenylyl cyclase; Hypercapnia

*Corresponding author at: Department of Pediatrics, Division of Neonatology, Johns Hopkins Medical University, 600 N. Wolfe Street, CMSC 6-104, Baltimore, MD 21287-3200, USA. Tel.: +1 410 614 7232. egauda@mail.jhmi.edu, egauda@jhmi.edu (E.B. Gauda).

1. Introduction

Peripheral arterial chemoreceptors located in the carotid body (CB) and central chemoreceptors located in the brainstem contain specialized cells that either depolarize in response to changes in P_aO_2 or in response to changes in CO_2/H^+. Type I (glomus) cells of the CB, the peripheral chemoreceptor units, are innervated by carotid sinus nerve (CSN) afferents, a branch of the glossopharyngeal nerve, which have somas in the petrosal ganglion (PG), and relay on to neurons in the nucleus tractus solitarius in the brainstem (Gonzalez et al., 1994). Although peripheral chemoreceptors were believed to be the major O_2 sensors while central chemoreceptors contributed predominantly to the CO_2/pH ventilatory response, recent evidence suggest that the central and peripheral chemoreceptors interact with each other, and the latter can modulate the central sensitivity to CO_2/pH (for a review see Forster and Smith (2010)). Accordingly, it is now recognized that preservation of functional CB activity is essential for mediating the full ventilatory response to hypercapnia. This emphasizes an important and fundamental homeostatic role for the CB in regulating the P_aCO_2 throughout the whole organism.

In the CB, transduction of the hypercapnic stimulus into a functional chemoafferent neural signal involves many of the same processes associated with hypoxia sensing. These include type I cell depolarization, Ca^{2+} influx and neurosecretion (reviewed in Kumar and Prabhakar, 2012). However, identification of the specific CO_2 sensing mechanisms in the type I cell required to activate the CB in response to hypercapnia, at present, remains incompletely defined. It is also unknown whether CO_2 sensing is mediated by CO_2/HCO_3^-, decreases in pH or both.

A crucial step in the CB hypercapnia transduction process appears to be the intracellular hydration of CO_2 to form HCO_3^- and H^+; a reaction catalyzed by carbonic anhydrase (CA) (Iturriaga et al., 1991; Travis, 1971; Zhang and Nurse, 2004). Increasing extracellular PCO_2 at constant HCO_3^- (acidic hypercapnia) is coupled with a reduction in intracellular pH (pH_i) in the type I cell (Buckler et al., 1991a). The steady state acidic pH_i observed in hypercapnia is reported to be dependent not only on intracellular CA mediated H^+ generation, but also on a concurrent extracellular acidosis, most probably by restricting H^+ extrusion (Buckler et al., 1991a,b). Initiation of type I cell depolarization in acidic hypercapnia has been suggested as being a consequence of an alteration in the H^+ sensitive TASK-like (Buckler et al., 2000; Buckler and Vaughan-Jones, 1994) and acid-sensing (Tan et al., 2007) ion channel currents.

In contrast to this ‘acid’ hypothesis, it has also been observed that in some in vitro CB preparations an increase in extracellular PCO_2 and HCO_3^-, without altering the pH_o (isohydric hypercapnia), can stimulate a rise in the type I cell inward Ca^{2+} current (Summers et al., 2002), augment cellular neurotransmitter release (Rigual et al., 1991) and activate chemoafferent fibers in the CSN (Zhang and Nurse, 2004). These observations are consistent with some of the excitatory mechanisms induced by hypercapnia being independent of concurrent acidosis. Furthermore, augmentation of the inward Ca^{2+} current in isohydric hypercapnia has been proposed to be dependent on an increase in cAMP leading to the upregulation of protein kinase A (PKA) activity (Summers et al., 2002). Taken

together, these observations suggest that the CB senses independently both HCO_3^- and H^+, but the specific target for CO_2/HCO_3^- remains unknown.

Since we had recently identified HCO_3^--sensitive soluble adenylyl cyclase (sAC) in the CB, we hypothesized that sAC could be a sensor for rapid changes in [CO_2]. Thus, the importance of the present work is to investigate the function of sAC in the CB, through its activation by isohydric hypercapnic conditions, and clarify the mechanism of hypercapnia detection in this organ.

Two types of adenylyl cyclases mediate the production of cAMP in mammalian cells: the family of transmembrane adenylyl cyclase (tmAC) isoforms and sAC. At least nine specific tmAC isoforms have been identified in mammalian genomes, but they have not yet been characterized in the CB. tmAC isoforms are sensitive to G-protein, forskolin (FSK), Ca^{2+}-signaling pathways (Halls and Cooper, 2011) and CO_2 (Cook et al., 2012; Townsend et al., 2009). In the CB, it is established that cellular cAMP levels can be modulated by neurotransmitters/neuromodulators that bind to G-protein coupled receptors (GPCR) and alter tmAC activity (Gonzalez et al., 1994; Lahiri et al., 2006). Whether neurotransmitter/neuromodulator or direct CO_2 induced activation of tmAC occurs in hypercapnia independent of acidosis is investigated in this study.

sAC is activated by HCO_3^- (bicarbonate ion) and Ca^{2+} (reviewed by Kamenetsky et al., 2006). Thus we hypothesized that sAC may be stimulated directly in hypercapnia by a rise in HCO_3^- subsequent to the CA mediated hydration of CO_2. We have previously identified sAC mRNA and protein in the CB and related peripheral non-chemosensitive structures (Nunes et al., 2009). In this article we examine whether sAC is functionally active in the CB and has a role in the chemotransduction process of hypercapnia, independent of concurrent extracellular and therefore intracellular acidosis. Thus, in this work we study tmAC and sAC activity in isohydric hypercapnia to assess whether increases on cAMP levels in the CB in response to hypercapnia are mediated by CO_2/HCO_3^- or decreases in pH.

2. Materials and methods

2.1. Animals and surgical procedures

The Animal Care and Use Committee at the Johns Hopkins University School of Medicine approved all experimental protocols. CSN recording experiments were performed at University of Birmingham and were approved by the Biomedical Services Unit.

All tissues (CB and PG) were isolated from Sprague-Dawley rats (SD, Charles River Laboratories, Wilmington, MA) of both sexes.

In one set of experiments, prior to tissue removal or dissection, the animals at postnatal days (P) 16 and 17 were anesthetized briefly with isoflurane and immediately decapitated. At this age, CB hypoxic chemosensitivity is mature (Kholwadwala and Donnelly, 1992). The carotid bifurcation, including the CB, superior cervical ganglia, and the nodose/petrosal ganglia complex, was removed *en bloc*. CBs and PGs were subsequently isolated and cleaned of surrounding connective tissue under a dissecting microscope. In another set of experiments, we dissected CB for dissociation of type I cells from SD rats at P5–9. At this

age dissociated cells were easier to obtain and no statistical differences ($p = 0.1143$, Mann–Whitney test) in cAMP accumulation were observed between the whole CB from rats P7 (23.5 ± 3.1 fmol/μg protein, $n = 6$) and P17 (33.9 ± 4.6 fmol/μg protein, $n = 4$) in normocapnic conditions.

Lastly, CSN recording experiments were performed with tissues obtained from adult male SD rats (50–100 g, Charles River UK, Ltd., Margate, UK). CBs were harvested as described previously (Pepper et al., 1995). Briefly, anesthesia was induced in an airtight induction chamber using 4% isoflurane in medical O_2 administered at a flow rate of 1.5–3 ml/min. Surgical anesthesia was continuously maintained through a nose cone with 1.5–2.0% isoflurane in O_2, at a flow rate of 1.5–3 ml/min. The carotid bifurcation along with the superior cervical ganglion, vagus nerve, glossopharyngeal nerve, CSN, and the CB were all excised. The tissue was immediately placed in ice-cold HCO_3^- buffered extracellular Krebs solution containing (in mM): 125 NaCl, 3 KCl, 1.25 NaH_2PO_4, 5 Na_2SO_4, 1.3 $MgSO_4$, 24 $NaHCO_3$, 2.4 $CaCl_2$, 11 D-glucose, equilibrated with 95% O_2 and 5% CO_2.

2.2. sAC and tmAC mRNA gene expression

The mRNA expression levels for sAC and the nine isoforms of tmAC in the CB and PG were compared. The tissues were isolated as discussed for surgical procedures (4 rats per condition; $n = 3$ independent experiments), cleaned from surrounded tissue, frozen on dry ice, and stored at −80 °C until further processing for quantitative Real-Time PCR, as outlined below.

2.3. Quantitative Real-Time (qRT) PCR

Tissues used to determine the level of sAC and tmAC mRNA gene expression were processed to obtain total RNA (Micro-to-Midi Total RNA Purification, Invitrogen, Carlsbad, CA) according to the manufacturer's instructions. DNase treatment (PureLink DNase, Invitrogen) was performed to avoid genomic DNA contamination. RNA yield and quality was measured at 260 and 280 nm using a UV spectrophotometer (Beckman Du 530) or NanoDrop spectrophotometer (for RNA from CB samples, Thermo Scientific, Wilmington, DE). Total RNA (about 1 μg) was used for first-strand cDNA synthesis using an iSCRIPt cDNA synthesis kit (Bio-Rad Laboratories, Hercules, CA).

The primer sequences for each adenylyl cyclase isoform used are shown in Table 1 (Chang et al., 2003; Pastor-Soler et al., 2003). Relative expression levels for adenylyl cyclase genes between tissues and conditions were standardized using the reference gene glucose-6-phosphate dehydrogenase (G6PDH). Results were further validated using two additional reference genes: glyceraldehyde 3-phosphate dehydrogenase (GAPDH) and beta-actin (β-actin). The primer sequences for the reference genes used are presented in Table 1 (Wang and Xu, 2010). The expression of the three reference genes in all the tissues used and conditions was evaluated by combining four different algorithms used to determine the stability of the reference genes: geNorm, Normfinder, Bestkeeper, and the comparative ΔC_T method (http://www.leonxie.com/referencegene.php?type=reference).

qRT-PCR was performed using a MyiQ iCycler RT-PCR system (Bio-Rad) with the SYBR Green detection system. Each PCR reaction consisted of 1 μl of cDNA and 3.5 μl of 300 nM primers diluted in DEPC-H_2O and 10 μl of SYBR Green Supermix (Bio-Rad) for a final volume of 20 μl. Triplicates were performed for each sample. PCR conditions for adenylyl cyclase (tmAC and sAC) expression were: denaturing 5 min at 95 °C, followed by 40 cycles at 95 °C for 20 s, 62 °C for 20 s, 72 °C for 20 s, and a terminal extension period (72 °C, 10 min). The specificity of the RT-PCR product was analyzed by performing a melting curve with 0.5 °C increments in temperature. Product formation during the exponential phase of the reaction was analyzed for relative quantification to reference gene based on the threshold cycle (C_T) for amplification as $2^{(\Delta C_T)}$, where $\Delta C_T = C_{T,reference} - C_{T,target}$.

2.4. Intracellular pH measurement in carotid body

Intracellular pH (pH_i) was measured using the pH-sensitive fluorescence dye, BCECF-AM (Molecular Probes, Eugene, OR) using a protocol previously described by Iturriaga et al. (1992). The isolated CB was incubated with trypsin (0.02%, Sigma) and collagenase (0.01%, Sigma) for 30 min, and rinsed in phosphate buffered saline (PBS). The CB was incubated with BCECF-AM (5 μM) at 37 °C for 1 h and washed to remove excess dye. Since type I cells, the sensors of the CB, appear usually in clusters, these regions were selected as the regions of interest (ROI) and were analyzed for changes in BCECF-AM fluorescence intensity while the whole organ was superfused with oxygenated solutions containing increasing concentrations of HCO_3^-/CO_2. All solutions were titrated to pH 7.4 as described above. Fluorescent images were examined with a fluorescent microscope (Nikon Eclipse E-400, Nikon Instruments, Melville, NY) and captured at 400× with an attached charge-coupled device (CCD) camera (Hamamatsu, Photonic ItSystems, Bridgewater, NJ). The BCECF dye was excited at 495 nm and emission was recorded at 519 nm. The images were captured over a period of 200 frames corresponding to 2.38 min and analyzed using Ivison (BioVision Technologies, PA). To avoid photobleaching, the intensity of light was controlled by Exfo X-cite 1200PC (0.12 intensity, Exfo Photonic Solutions, Ontario, Canada). A calibration curve for each CB was performed at the end of each experiment using the nigericin (10 μM)/high K^+ method (Thomas et al., 1976) to determine changes in fluorescence intensity versus pH (6.5–8.0). Exposure to ammonium chloride (NH_4Cl, 50 mM) was used to ensure that dye intensity corresponded to changes in intracellular pH (Buckler et al., 1991b).

2.5. Contribution of sAC and tmAC on cAMP levels in response to different concentrations of HCO_3^-/CO_2 (normocapnic and isohydric hypercapnic conditions)

In one set of experiments, we pre-incubated CB in Krebs modified solution containing (in mM): NaCl 135, KCl 5, $CaCl_2$ 2, $MgCl_2$ 1.1, Hepes 10, glucose 5.5, pH 7.40 (Peréz-García et al., 1990) without HCO_3^-/CO_2 in the absence and presence of the tmAC inhibitor, 2′5′-ddADO (100 μM) or sAC inhibitor, KH7 (50 μM) or both for 30 min. The CBs were subsequently transferred to a fresh incubation buffer for 30 min, in normocapnic and isohydric hypercapnic conditions, in the absence and presence of the tmAC inhibitor, 2′5′-ddADO (100 μM) or sAC inhibitor, KH7 (50 μM) or both.

In another set of experiments, we tested the effect of the tmAC selective inhibitor, 2′5′-ddADO (100 μM, Sigma), or sAC inhibitor, KH7 (10 μM, Sigma), separately or together on the cAMP accumulation in the CB over time (0, 5, 15 and 30 min of incubation) under normocapnic and isohydric hypercapnic conditions. We pre-incubated the CBs in Krebs modified solution without HCO_3^-/CO_2 or containing either 24 mM $HCO_3^-/5\%CO_2$ or 44 mM $HCO_3^-/10\%CO_2$ in the absence or presence of the adenylyl cyclase inhibitors for 30 min. Then, the CBs were placed in fresh incubation buffer without HCO_3^-/CO_2 or containing either 24 mM $HCO_3^-/5\%CO_2$ or 44 mM $HCO_3^-/10\%CO_2$, in the presence of a non-specific inhibitor for phosphodiesterase (PDE), IBMX (500 μM, Sigma) and in the absence or presence of adenylyl cyclase inhibitors, for 0, 5, 15 and 30 min. The incubation buffer was modified by changing CO_2 and HCO_3^- concentrations and adjusting the osmolarity with NaCl. This approach allowed the assessment of any HCO_3^-/CO_2 effect while keeping extracellular pH constant. All the experiments were done in the presence of $60\%O_2$ since hypoxia has been known to increase the chemosensitivity response to CO_2 (Fitzgerald and Parks, 1971).

2.6. Cyclic nucleotide extraction and quantification

cAMP was measured as previously reported (Batuca et al., 2003). Briefly, tissues were immersed in cold 6% (w/v) trichloroacetic acid (600 μl) for 10 min, and then the tissues were homogenized at 2–8 °C and centrifuged at 12,000 × *g* for 10 min at 4 °C. The pellet was washed four times in 3 ml of water saturated with diethyl ether solution (50:50) and then lyophilized. The sample was stored at −20 °C until cAMP quantification by enzyme immunoassay (EIA, RPN 2255, GE Healthcare Bio-Sciences AB, Piscataway, NJ). Protein pellets were stored at −20 °C until measured with a fluorescence detection kit, NanoOrange Protein (Invitrogen, Eugene, OR). cAMP levels were expressed in femtomoles per microgram of protein (fmol/μg protein), which is more accurate than normalizing to grams of tissue, especially for small tissue samples, such as the CB.

2.7. Changes in protein kinase A (PKA) activity in dissociated type I cells of the CB using FRET-based sensors

CBs isolated from SD rats P5–9 were mechanically and enzymatically dissociated with an enzyme mixture consisting of trypsin and collagenase (~0.5 mg/ml) according to the protocol described by Carroll et al. (2005). CB cells were plated on poly-D-lysine coated imaging dishes and cultured for 3 h. A 3rd generation genetically encoded A-Kinase activity reporter dependent on FRET (AKAR3) was used to monitor PKA activity. AKAR3 consists of a fusion of CFP, a phosphothreonine-binding domain, a PKA substrate, and the YFP variant venus (Allen and Zhang, 2006). When PKA is activated, the catalytic subunit of PKA phosphorylates the target in AKAR3, causing a conformational reorganization that increases FRET between CFP and YFP (Allen and Zhang, 2006). Adenoviruses expressing the AKAR3 reporter were obtained from Yang K. Xiang's laboratory and infected into the CB type I cells for 24 h. One hour before FRET imaging, CB type I cells were labeled with rhodamine PNA (Rho-PNA, 30 μg/ml) in complete CB medium at 37 °C as previously described by Kim et al. (2009). After an hour, the imaging dish containing the cells infected with AKAR3 and labeled with Rho-PNA was placed into a chamber (Warner Instruments, Hamden, CT) to allow superfusion of the cells with a constant flow rate of 2 ml/min

(Ismatec, Cole Parmer instrument CO, Vernon Hills). The cells were imaged on a Zeiss Axiovert 200 M microscope (Carl Zeiss, Thornwood, NY) with a 40× oil immersion objective and a cooled charge-coupled device camera (Roper Scientific, Trenton, NJ) controlled by Metafluor 6.2 software (Molecular Deices, Downingtown, PA). Dual emission ratio imaging used a 420DF20 excitation filter, a 450DRLP dichroic mirror and two emission filters (475DF40 for CFP and 535DF25 for YFP). Exposure time was 50–500 ms and images were acquired every 20 s. Background correction of the fluorescence images was performed by subtracting intensities from regions of the imaging dish with no cells. To test the contribution of tmAC and sAC to PKA activity, CB cells were incubated in the presence of sAC and tmAC activators, HCO_3^-/CO_2 (0/0–44/10 mM/%) and FSK (50 μM), respectively. PDEs were inhibited by IBMX (10 μM). Graph curves were normalized by setting the emission ratio before drug addition equal to one.

In a subset of experiments we identify type I cells by tyro-sine hydroxylase (anti-TH mouse monoclonal antibody, 1:50, and detected with goat anti-mouse secondary antibody, 1:100) and fluoresceinated peanut agglutin (rho-PNA) staining and confirmed that those cells expressed A-Kinase activity reporter (AKAR3).

2.8. Extra-cellular CSN recordings

The carotid bifurcation, along with the superior cervical ganglion, vagus nerve, glossopharyngeal nerve, CSN, and the CB were pinned out in a small volume (ca. 0.2 ml) dissecting chamber with a Sylgard 184 base (Dow Corning). The tissue was continuously superfused with a bicarbonate buffered extracellular Krebs solution containing (in mM): 125 NaCl, 3 KCl, 1.25 NaH_2PO_4, 5 Na_2SO_4, 1.3 $MgSO_4$, 24 $NaHCO_3$, 2.4 $CaCl_2$, 11 D-glucose, equilibrated with 95% O_2 and 5% CO_2. Connective tissue was removed and the superior cervical ganglion, branches of the vagus nerve and the occipital artery were all individually excised. The CSN was cut away from the glossopharyngeal nerve exposing the nerve endings. The whole tissue was partially digested by incubation in a bicarbonate buffered, equilibrated 95% O_2 and 5% CO_2 enzyme solution (0.075 mg/ml collagenase type II, 0.0025 mg/ml dispase type I; Sigma) at a temperature of 37 °C, for 20–30 min, in a water bath at 37 °C (Grant W14, Grant Instruments Cambridge, Ltd.).

Extracellular recordings were made from the cut end of the CSN using glass suction electrodes pulled from GC150-10 capillary glass (Harvard Apparatus). Voltage was amplified using an AC pre-amplifier (NeuroLog NL104; Digitimer) then filtered between 50 Hz and 3 kHz (NeuroLog NL125; Digitimer) and amplified further with an AC amplifier (NeuroLog 105; Digitimer). The total amplification was 4000×. Derived voltage was recorded using a CED micro1401 (Cambridge Electronic Design) and visualized on a PC with Spike2 (version 7.1) software (Cambridge Electronic Design). Offline analysis using Spike2 allowed for discrimination of single unit activity.

Flow meters with high precision valves (Cole Palmer Instruments) were used in order to gas the superfusate with a desired gas mixture. The superfusate PO_2 was continuously measured using an O_2 meter (OXELP, World Precision Instruments) and was maintained throughout at 300 mm Hg. The superfusate PCO_2 was increased from 40 mm Hg with 24 mM $NaHCO_3$ to 80 mm Hg with 44 mM $NaHCO_3$ to monitor CB responses to isohydric hypercapnia, or

from 40 to 80 mm Hg, both in the presence of 24 mM $NaHCO_3$ to monitor CB responses to acidic hypercapnia. Osmolality was balanced by reducing the NaCl concentration.

2.9. Data analysis and statistical procedures

The data are represented as mean ± SEM and differences between the experimental groups were determined using statistical software from GraphPad Prism (GraphPad Software Inc., version 4, San Diego, CA) or SPSS (SPSS Inc., version 12, Chicago, IL). Statistical significance was set at $p < 0.05$.

3. Results

3.1. sAC and tmAC (I–IX isoforms) gene expression

mRNA levels for sAC and the 9 tmAC isoforms were quantified in the CB and PG. As previously observed (Nunes et al., 2009), we confirmed that sAC expression was higher in the CB than in the PG ($p < 0.05$, Fig. 1). In the CB, relative gene expression for the isoforms: tmAC1 (Ca^{2+} and calmodulin stimulated), tmAC4 (G-protein Gβγ stimulated), tmAC6 (PKA, PKC and Ca^{2+} inhibited) and tmAC9 (Ca^{2+} inhibited) were significantly greater than sAC ($p < 0.001$, Fig. 1). We observed that the CB and PG expression profile for the 9 tmAC isoforms (Fig. 1) differed; tmAC1 (Ca^{2+} and calmodulin stimulated), tmAC4 (Gβγ stimulated), and tmAC6 (PKA, PKC and Ca^{2+} inhibited) was higher in the CB than in the PG ($p < 0.001$, Fig. 1), while the levels of tmAC2 (Gβγ and PKC stimulated) were lower ($p < 0.001$, Fig. 1). tmAC3 and tmAC8 (calmodulin-Ca^{2+} stimulated), tmAC5 and tmAC7 (PKC-stimulated), and tmAC9 (Ca^{2+}-inhibited) gene expression did not differ between tissues. These results demonstrated that even though sAC mRNA is highly expressed in the CB, it is much lower than of the level of expression for tmAC.

3.2. sAC and tmAC inhibition in isohydric hypercapnia

We previously reported that, when tmAC was inhibited by MDL-12,330 A (500 μM, IC_{50} = 250 μM (Guellaen et al., 1977)), increasing HCO_3^-/CO_2 from 0/0 to 24/5 (mM/%) HEPES based Krebs solution in the presence of IBMX (500 μM) augmented cAMP levels in the CB from 15.3 ± 3.2 ($n = 16$) to 35.3 ± 6.0 ($n = 14$) fmol/μg protein ($p < 0.01$) but not in peripheral non-chemosensitive tissues (Nunes et al., 2009). Higher concentrations of HCO_3^-/% CO_2 (44 mM/10%) did not produce additional increase in cAMP levels in this tissue (Nunes et al., 2009). In the present work, additional experiments including 12 mM HCO_3^-/2.5% CO_2 confirmed an increase in cAMP levels from 0/0 to 12/2.5 and to 24/5 (mM/%), with no changes of cAMP levels in the presence of isohydric hypercapnia (Supplemental Fig. 1).

Supplementary data associated with this article can be found, in the online version, at http://dx.doi.org/10.1016/j.resp.2013.05.013.

To determine whether the changes in cAMP levels in response to different concentrations of HCO_3^-/CO_2 were mediated by a direct effect of bicarbonate or due to changes in intracellular pH (pH_i) in the CB, we measured pH_i using the pH-sensitive fluorescence dye BCECF-AM. A control experiment with NH_4Cl showed that there was a distinct change in

fluorescent intensity in the cells of the CB (Fig. 2A and B). Furthermore, incremental changes in fluorescent intensity associated with changes in extracellular pH (6.5–8.0) were observed using the nigericin (10 μM)/high K^+ method to construct calibration curves. No variation in pH_i associated with changes from 0 mM HCO_3^-/0% CO_2 to 44 mM HCO_3^-/10% CO_2 within each selected region of the whole CB was observed (Fig. 2C and D). These results suggested that increases in HCO_3^-/CO_2 with constant extracellular pH did not change pH_i in our experimental preparations.

Although we had observed that MDL-12,330 A was effective blocking tmAC in our preparations suggesting little contribution of sAC when tmAC is activated by forskolin (Supplemental Fig. 2) (Delpiano and Acker, 1991), we did not find evidence in literature about its selectivity for tmAC relative to sAC. To study the selectivity of this inhibitor, we compared its effect with other tmAC inhibitors: 2′5′-ddADO (30–300 μM, IC_{50} = 3–16 μM (Ramos et al., 2008) and SQ 22536 (200 μM, IC_{50} = 20 μM (Rocher et al., 2009), and sAC inhibitor KH7 (10–100 μM, IC_{50} = 2–5 μM (Ramos et al., 2008)) on cAMP production during isohydric hypercapnia. MDL-12,330 A (500 μM) blocked cAMP production by 96.1 ± 0.4% (n = 22, Supplemental Fig. 3). Other tmAC specific inhibitors, 2′5′-ddADO (100 μM, 60.0 ± 10.5% of inhibition, n = 6, Supplemental Fig. 3) and SQ 22536 (200 μM, 63.0 ± 3.5% of inhibition, n = 3, Supplemental Fig. 3) had less of an impact on blocking cAMP production compared with MDL-12,330 A, suggesting either that the latter may not be a specific tmAC inhibitor at this high concentration or that cAMP production could be mainly due to tmAC activation. KH7 blocked cAMP production in a concentration-dependent manner (10 μM of KH7 blocked cAMP levels by 6.9 ± 13.0%, n = 9; 50 μM by 60.7 ± 13.0%, n = 9; 100 μM by 69.4 ± 6.7%, n = 8, Supplemental Fig. 3).

Supplementary data associated with this article can be found, in the online version, at http://dx.doi.org/10.1016/j.resp.2013.05.013.

3.3. From normocapnia to isohydric hypercapnia: relative contribution of sAC and tmAC to cAMP accumulation

To investigate if these enzymes have a role in HCO_3^-/CO_2 sensing in the CB, we compared the effect of an equipotent concentration of tmAC and sAC inhibitors (100 μM of 2′5′-ddADO and 50 μM of KH7). We pre-incubated CB tissue in the absence and presence of the tmAC inhibitor, 2′5′-ddADO (100 μM) or sAC inhibitor, KH7 (50 μM) or both, during 30 min, in normocapnic and isohydric hypercapnic conditions.

2′5′-ddADO (100 μM) reduced whole CB cAMP content by 55.1 ± 5.5% (n = 8) under normocapnia and by 55.3 ± 6.7% (n = 10) under isohydric hypercapnic conditions. KH7 (50 μM) decreased cAMP by 30.81 ± 8.5% (n = 4) and by 43.1 ± 9.2% (n = 4) under normocapnia and isohydric hypercapnia conditions, respectively. No differences were observed in the presence of both KH7 (50 μM) and 2′5′-ddADO (100 μM) between these two conditions (33.4 ± 10.8 (n = 4) and 25.4 ± 11.7 (n = 4) under normocapnia and isohydric hypercapnia conditions, respectively). These results suggested that the level of depression in cAMP accumulation induced by sAC or tmAC inhibition does not change significantly between normocapnia and isohydric hypercapnia, and thus, sAC or tmAC activity is not up regulated in response to isohydric hypercapnia.

Since sAC is directly activated by HCO_3^-/CO_2 while tmAC can be activated by neurotransmitters released by the cells that bind to G-protein coupled receptors, we postulated that sAC could be activated earlier than tmAC. We explored this hypothesis by determining the time course (0, 5, 15, 30 min) of cAMP production. cAMP levels were assessed after a 30 min pre-incubation without HCO_3^-/CO_2 or containing either 24 mM HCO_3^-/5% CO_2 or 44 mM HCO_3^-/10% CO_2, taken as the 0 min time point, with subsequent measurements after 5, 15 or 30 min, in an incubation media without HCO_3^-/CO_2 or during normocapnic and isohydric hypercapnic conditions, in the presence of IBMX and in the presence or absence of adenylyl cyclase inhibitors. After a pre-incubation of 30 min, no changes in cAMP levels were found over time up to 30 min in an incubation media containing 24 mM HCO_3^-/5% CO_2 or 44 mM HCO_3^-/10% CO_2, in the absence and presence of AC inhibitors and IBMX (Fig. 3A and B). These findings suggest to us that changes in HCO_3^-/CO_2 in the presence of a phosphodiesterase inhibitor did not increase cAMP levels after pre-incubation and sAC is not contributing to an increase in cAMP in response to changes in HCO_3^-/CO_2, even in more acute conditions.

3.4. Changes in protein kinase A (PKA) activity in dissociated type I cells of the CB

As the CB O_2/CO_2 sensors are located in type I cells, we explored whether the lack of effect of isohydric hypercapnia on cAMP accumulation observed in the whole CB was consistent with modulation of downstream targets of cAMP in isolated type I cells. Thus, we determined the effect of different concentrations of HCO_3^-/CO_2 on PKA activity in type I cells of the CB using a genetically encoded AKAR3 reporter dependent on FRET. We confirmed the co-localization of Rho-PNA with tyrosine hydroxylase (Fig. 4.1), and co-localization of Rho-PNA with AKAR3 virus expression in type I cells of the CB (Fig. 4.2). Cells were perfused with medium containing 0 mM HCO_3^-/0% CO_2, followed by application of a sub-maximal concentration of IBMX (10 μM) to avoid saturation of the reporter, which increased FRET emission ratio by 6.0 ± 4.8% (n = 21 cells). IBMX (10 μM) was maintained through the experiment and the perfusate was changed from 0 mM HCO_3^-/0% CO_2 to 24 mM HCO_3^-/5% CO_2 or to 44 mM HCO_3^-/10% CO_2 with no observed change in FRET emission ratio (Fig. 5). Addition of FSK (50 μM) markedly increased the emission ratio to 7.4 ± 1.1%. H89 (10 μM, IC_{50} = 50 nM (Rocher et al., 2009)), a PKA inhibitor, decreased the emission ratio by 14.6 ± 1.4% (n = 21, Fig. 5A–C). These results demonstrate that PKA activity is independent of HCO_3^- concentration. These results are consistent with the measurements of cAMP in the whole CB and suggest that isohydric hypercapnia does not increase PKA activity in type I cells.

3.5. The impact of isohydric hypercapnia on chemoafferent carotid sinus nerve activity

Since isohydric hypercapnia did not induce a change on cAMP-PKA levels, we examined if there was any functional impact of isohydric hypercapnia on the CSN chemoafferent discharge frequency. A characteristic raw trace example is demonstrated in Fig. 6A. Analysis of grouped data showed that the single fiber frequency measured in normocapnia (PCO_2 ~ 40 mm Hg, HCO_3^- ~ 24 mM) was significantly augmented by acidic hypercapnia (PCO_2 ~ 80 mm Hg, HCO_3^- ~ 24 mM) but not by isohydric hypercapnia (PCO_2 ~ 80 mm Hg, HCO_3^- ~ 44 mM) (n = 6, Fig. 6B). These findings are consistent with the notion that activation of the CSN chemoafferents in response to a rise in PCO_2 is critically dependent

on a decrease in extracellular pH (that acts to maintain the hypercapnia induced steady state intracellular acidosis), as previously suggested by others (Buckler et al., 1991a; Gray, 1968; Lahiri et al., 1996).

4. Discussion

The present results show that sAC does not have any physiologically significant role in cAMP production in response to isohydric hypercapnia in the carotid body since: (1) sAC relative mRNA expression is lower than tmACs (Fig. 1), (2) no time-dependent changes in cAMP, in the presence or absence of KH7 (sAC blocker), from 0 mM HCO_3^-/0%CO_2 to 44 mM HCO_3^-/10%CO_2 were observed (Fig. 3) and (3) no effect on PKA activity in the presence of different concentrations of HCO_3^-/CO_2 was observed (Fig. 5). These results suggest that the enhanced cAMP generation and CB chemoafferent discharge frequency associated with an increase in CO_2 is not mediated directly by CO_2 or HCO_3^- but is probably a consequence of a concurrent elevation in intracellular and extracellular H^+ generation.

The CO_2-sensing mechanism in the CB is not fully understood. CO_2, H^+ and HCO_3^- are intimately connected yet the nature of the primary stimuli remains uncertain. Some studies in the CB have demonstrated that this mechanism is mediated via decreasing extracellular or intracellular pH (pH_i), leading to a membrane depolarization, which can be mediated by TASK channels (Buckler et al., 2000) or acid channels (Tan et al., 2007). Membrane depolarization leads to an activation of calcium channels with concomitant increase in intracellular calcium levels and neurotransmitter release (Buckler and Vaughan-Jones, 1994). Acidosis can also activate Na^+/H^+ exchange promoting the reversal of Na^{2+}/Ca^{2+} exchange, which results in elevated intracellular calcium concentrations (Rocher et al., 1991). CO_2/HCO_3^- (isohydric hypercapnia) has been reported to be directly involved in the activation of Ca^{2+} currents leading to an increase of intracellular Ca^{2+} (Summers et al., 2002). Once in the cell, CO_2 is in dynamic equilibrium with HCO_3^- and pH, through the reaction catalyzed by carbonic anhydrases (Ridderstråle and Hanson, 1984). It has been proposed that carbonic anhydrase function influences the CB sensitivity to CO_2/pH (Iturriaga et al., 1993; Lahiri and Forster, 2003). Thus increases in CO_2 could lead to increases in HCO_3^- that could activate sAC (Chen et al., 2000) and consequently increase cAMP levels. Our group had previously identified the expression of sAC gene in the CB and suggested a functional role for sAC in this organ since: (1) sAC gene expression levels in the CB were at least 10 times higher than in non-chemoreceptors, except testis, a tissue where high levels of sAC have been observed; (2) sAC mRNA levels in the CB were up-regulated by HCO_3^-/CO_2, (3) sAC protein was present in the CB and (4) cAMP levels increased with augments in HCO_3^-/CO_2 from 0/0 to 24/5 (Nunes et al., 2009). Other than the CB, the role for sAC has been described in tissues where changes in HCO_3^-/CO_2 are essential to their function. For instance, in the testis, where sAC is highly expressed, sAC mediates sperm maturation and acquisition of motility, in kidneys it regulates recycling of V-ATPse, in airway epithelial cells sAC regulates the ciliary beat frequency, and in corneal endothelium it plays a role in the activation of the cystic fibrosis transmembrane conductance regulator, among others (Buck et al., 1999; Chen et al., 2000; Hess et al., 2005;

Pastor-Soler et al., 2003; Schmid et al., 2007; Sun et al., 2004). The role of sAC in CO_2/HCO_3^- sensing has never been studied in the CB chemoreceptors.

cAMP levels can also be synthesized by tmAC. Recently, it was demonstrated that tmAC activity is modulated by CO_2 (Townsend et al., 2009). Since it has been suggested that, in the CB, cAMP levels increase in response to acidic and possibly isohydric hypercapnia (Peréz-García et al., 1990; Summers et al., 2002), it was of interest to understand the role of tmAC and sAC in the CO_2/HCO_3^- sensing mechanism of the CB.

We characterized for the first time the nine tmAC isoforms (tmAC1–9) in the CB and PG. Differences in the tissue distribution of the different isoforms were observed with a predominance of the expression of tmAC versus sAC in both tissues. The information available in the literature is not sufficient to allow a correlation between AC mRNA profiles and specific G-protein and consequently specific GPCR. D2-dopamine and M2-muscarinic receptors, which inhibit tmAC, have been identified in both PG and CB (Alcayaga et al., 1999; Bairam et al., 2006; Gonzalez et al., 1994). A2 adenosine receptors and adrenergic β-receptors, which are positively coupled to tmAC, are present in the CB (Gauda, 2002; Gonzalez et al., 1994). While β-adrenergic and D2 dopamine receptors in heart and striatum are coupled to tmAC5 (Chern, 2000; Sadana and Dessauer, 2009) in the CB and PG these receptors would have to be coupled to a different tmAC isoform because we here demonstrate that tmAC5 is not expressed in the PG and CB.

In order to isolate the stimulus to better understand the CO_2/HCO_3^- chemosensitivity with pH controlled in the CB, and although it is far from being physiological, we study the effect of isohydric hypercapnia in tmAC and sAC activities. Although tmAC and sAC were expressed and functional in the CB, the results presented here suggested that the increases in cAMP levels in response to isohydric hypercapnia suggested by others (Summers et al., 2002) could not be directly attributed to increases in sAC and tmAC activity mediated by CO_2/HCO_3^-. sAC and tmAC inhibitors did not alter cAMP levels between normocapnia and isohydric hypercapnia. Also, in the absence of adenylyl cyclase inhibitors, cAMP levels did not increase in response to HCO_3^-/CO_2 concentrations either after 5 or 30 min of incubation. PKA activity did not change with isohydric hypercapnia.

Peréz-García et al. (1990) described that increases in cAMP levels mediated by CO_2 were associated with decreases in intracellular pH. However our results were not dependent on decreases in intracellular pH with CO_2 since we designed our experiments to maintain the extracellular pH constant at 7.4 in all solutions and confirmed that exposure to different concentrations of HCO_3^-/CO_2 did not modify intracellular pH (Supplemental Fig. 3). It is known that when extracellular pH remains constant minimal changes are observed in pH_i of type I cells; when PCO_2 increases, pH_i transiently decreases and then rapidly equilibrates to the extracellular pH (Buckler et al., 1991a). Hornbein and Roos reported in 1963 that HCO_3^- and CO_2 do not affect pH_i in type 1 cells (see in Wilding et al., 1992). Furthermore, pH varying from 7.0 to 8.0 does not alter sAC mRNA expression (Sun et al., 2004). sAC enzyme activity is also *independent* of pH_i (Chen et al., 2000).

In the present work, we also observed that an increase in CO_2/HCO_3^- was not essential to induce an increase in CSN discharge. Biscoe et al. (1970) had demonstrated that isohydric hypercapnia induced an increase in cat CSN discharge; however, for $PaCO_2$ up to 60 mm Hg the discharge in their experiments seemed to plateau. Buckler et al. (1991) had demonstrated that changes in PCO_2 at constant extracellular pH caused rapid transient changes in pHi but did not affect steady-state pHi. However, using our preparation we believe that this transient change is not enough to induce neurotransmitter release from type I cells and consequent CSN depolarization.

All together, isohydric hypercapnia causes no change in sAC or tmAC activity, which translates into no change in cAMP, PKA or discharge frequency. Thus, we propose that, for cAMP levels to increase in response to increases in PCO_2 as observed by others, intracellular and extracellular acid sensing may be necessary, but not CO_2/HCO_3^-, to lead to calcium dependent neurotransmitter release followed by K^+ channel inhibition to cause autocrine activation of GPCR and further activation of tmAC.

We quantified mRNA levels, pH_i and cAMP amounts in the whole CB, which preserves cell-cell interactions, but does not enable determination of the specific contribution of chemo and non-chemosensitive units within the CB. However, the results obtained measuring PKA activity using FRET based-reporters in isolated type I cells were consistent with those in the whole CB. Since the absence of response to HCO_3^-/CO_2 in PKA activity in P7 was consistent with the functional studies in P17 rats, we consider that the groups are comparable and the results obtained in the whole CB can be extrapolated to type I cells even though these experiments were done with animals at different postnatal ages. To our best knowledge, the effect of the development of the CB in the activity of the PKA has not been studied, however, in the rat hippocampus, there is evidence that the PKA activity and the subunit regulatory levels do not change between the first and third week of life (Karege et al., 2001).

We used 44 mM HCO_3^-/10% CO_2 as a hypercapnia condition, and since this lies outside the physiological range, we cannot exclude the possibility that the HCO_3^-/CO_2 transport mechanism could be saturated or that the HCO_3^-/CO_2 sensor may no longer be sensitive to such supra-physiological conditions. While these are limitations to our study design, we believe that our thorough approach of examining the contribution of sAC and tmAC on PCO_2 transduction at multiple levels (mRNA, PKA regulation, cAMP production and integrated chemodischarge) using robust pharmacological and novel (FRET) approaches has contributed to our understanding of this basic signaling pathway in carotid chemoreceptors.

In conclusion, we have shown that sAC and tmAC are active in the CB and postulate that they co-operate to maintain adequate cAMP levels in physiological conditions. In addition, we support the notion that a functional response to CO_2 requires a decrease in intracellular and extracellular pH suggested by others (Buckler et al., 1991a; Lahiri et al., 1996).

Supplementary Material

Refer to Web version on PubMed Central for supplementary material.

Acknowledgments

A.R. Nunes was supported by Science and Technology Foundation Fellowship (FCT, SFRH/BD/39473/2007). A.P.S. Holmes was supported by an A.E. Hills Scholarship from the University of Birmingham. This work was also financially supported by R01 HL 072748 (EBG) and R01 DK073368 (JZ). The authors would like to thank Dr. Yang K. Xiang for supplying the adenoviruses expressing the AKAR3 for FRET experiments. We would like to thank Insook Kim for her help and time to discuss protocols about dissociation and identification of type I cells.

Abbreviations

CB	carotid body
CA	carbonic anhydrase
IH	isohydric hypercapnia
CSN	carotid sinus nerve
PG	petrosal ganglion
sAC	soluble adenylyl cyclase
tmAC	transmembrane adenylyl cyclase
HCO_3^-	bicarbonate ion
PKA	protein kinase A
SD rats	Sprague-Dawley rats
P	postnatal days
FSK	forskolin
GPCR	G-protein coupled receptors

References

Alcayaga J, Varas R, Arroyo J, Iturriaga R, Zapata P. Dopamine modulates carotid nerve responses induced by acetylcholine on the cat petrosal ganglion in vitro. Brain Research. 1999; 831:97–103. [PubMed: 10411987]

Allen MD, Zhang J. Subcellular dynamics of protein kinase A activity visualized by FRET-based reporters. Biochemical and Biophysical Research Communications. 2006; 348:716–721. [PubMed: 16895723]

Bairam A, Joseph V, Lajeunesse Y, Kinkead R. Developmental pattern of M1 and M2 muscarinic gene expression and receptor levels in cat carotid body, petrosal and superior cervical ganglion. Neuroscience. 2006; 139:711–721. [PubMed: 16457956]

Batuca JR, Monteiro TC, Monteiro EC. Contribution of dopamine D2 receptors for the cAMP levels at the carotid body. Advances in Experimental Medicine and Biology. 2003; 536:367–373. [PubMed: 14635690]

Biscoe TJ, Purves MJ, Sampson SR. The frequency of nerve impulses in single carotid body chemoreceptor afferent fibres recorded in vivo with intact circulation. Journal of Physiology. 1970; 208:121–131. [PubMed: 5499750]

Buck J, Sinclair ML, Schapal L, Cann MJ, Levin LR. Cytosolic adenylyl cyclase defines a unique signaling molecule in mammals. Proceedings of the National Academy of Sciences of the United States of America. 1999; 96:79–84. [PubMed: 9874775]

Buckler KJ, Williams BA, Honore E. An oxygen-, acid- and anaesthetic-sensitive TASK-like background potassium channel in rat arterial chemoreceptor cells. Journal of Physiology. 2000; 525:135–142. [PubMed: 10811732]

Buckler KJ, Vaughan-Jones RD. Effects of hypercapnia on membrane potential and intracellular calcium in rat carotid body type I cells. Journal of Physiology. 1994; 478:157–171. [PubMed: 7965831]

Buckler KJ, Vaughan-Jones RD, Peers C, Lagadic-Gossmann D, Nye PC. Effects of extracellular pH PCO_2 and HCO_3^- on intracellular pH in isolated type-I cells of the neonatal rat carotid body. Journal of Physiology. 1991a; 444:703–721. [PubMed: 1822566]

Buckler KJ, Vaughan-Jones RD, Peers C, Nye PC. Intracellular pH and its regulation in isolated type I carotid body cells of the neonatal rat. Journal of Physiology. 1991b; 436:107–129. [PubMed: 2061827]

Carroll JL, Boyle KM, Wasicko MJ, Sterni LM. Dopamine D2 receptor modulation of carotid body type 1 cell intracellular calcium in developing rats. American Journal of Physiology: Lung Cellular and Molecular Physiology. 2005; 288:L910–L916. [PubMed: 15681393]

Chang LC, Wang CJ, Lin YL, Wang JP. Expression of adenylyl cyclase isoforms in neutrophils. Biochimica et Biophysica Acta. 2003; 1640:53–60. [PubMed: 12676354]

Chen Y, Cann MJ, Litvin TN, Iourgenko V, Sinclair ML, Levin LR, Buck J. Soluble adenylyl cyclase as an evolutionarily conserved bicarbonate sensor. Science. 2000; 289:625–628. [PubMed: 10915626]

Chern Y. Regulation of adenylyl cyclase in the central nervous system. Cellular Signalling. 2000; 12:195–204. [PubMed: 10781926]

Cook ZC, Gray MA, Cann MJ. Elevated carbon dioxide blunts mammalian cAMP signaling dependent on inositol 1,4,5-triphosphate receptor-mediated Ca^{2+} release. Journal of Biological Chemistry. 2012; 287:26291–26301. http://dx.doi.org/10.1074/jbc.M112.349191. [PubMed: 22654111]

Delpiano MA, Acker H. Hypoxia increases the cyclic AMP content of the cat carotid body in vitro. Journal of Neurochemistry. 1991; 57:291–297. [PubMed: 1711098]

Fitzgerald RS, Parks DC. Effect of hypoxia on carotid chemoreceptor response to carbon dioxide in cats. Respiration Physiology. 1971; 12:218–229. [PubMed: 4327983]

Forster HV, Smith CA. Contributions of central and peripheral chemoreceptors to the ventilatory response to CO_2/H^+ Journal of Applied Physiology. 2010; 108:989–994. http://dx.doi.org/10.1152/japplphysiol.01059.2009. [PubMed: 20075260]

Gauda EB. Gene expression in peripheral arterial chemoreceptors. Microscopy Research and Technique. 2002; 59:153–167. [PubMed: 12384960]

Gonzalez C, Almaraz L, Obeso A, Rigual R. Carotid body chemoreceptors: from natural stimuli to sensory discharges. Physiological Reviews. 1994; 74:829–898. [PubMed: 7938227]

Gray BA. Response of the perfused carotid body to changes in pH and PCO_2. Respiration Physiology. 1968; 4:229–245. [PubMed: 5643141]

Guellaen G, Mahu JL, Mavier P, Berthelot P, Hanoune J. RMI 12330 A, an inhibitor of adenylate cyclase in rat liver. Biochimica et Biophysica Acta. 1977; 484:465–475. [PubMed: 911855]

Halls M, Cooper DM. Regulation by Ca^{2+}-signaling pathways of adenylyl cyclases. Cold Spring Harbour Perspectives in Biology. 2011; 3:a004143.10.1101/cshperspect

Hess KC, Jones BH, Marquez B, Chen Y, Ord TS, Kamenetsky M, Miyamoto C, Zippin JH, Kopf GS, Suarez SS, Levin LR, Williams CJ, Buck J, Moss SB. The “soluble” adenylyl cyclase in sperm mediates multiple signaling events required for fertilization. Developmental Cell. 2005; 9:249–259. [PubMed: 16054031]

Iturriaga R, Mokashi A, Lahiri S. Dynamics of carotid body responses in vitro in the presence of CO_2–HCO_3^-: role of carbonic anhydrase. Journal of Applied Physiology. 1993; 75:1587–1594. [PubMed: 8282607]

Iturriaga R, Rumsey WL, Lahiri S, Spergel D, Wilson DF. Intracellular pH and oxygen chemoreception in the cat carotid body in vitro. Journal of Applied Physiology. 1992; 72:2259–2266. [PubMed: 1629081]

Iturriaga R, Lahiri S, Mokashi A. Carbonic anhydrase and chemoreception in the cat carotid body. American Journal of Physiology. 1991; 261:C565–C573. [PubMed: 1928321]

Kamenetsky M, Middelhaufe S, Bank EM, Levin LR, Buck J, Steegborn C. Molecular details of cAMP generation in mammalian cells: a tale of two systems. Journal of Molecular Biology. 2006; 362:623–639. [PubMed: 16934836]

Karege F, Lambercy C, Schwald M, Steimer T, Cissé M. Differential changes of cAMP-dependent protein kinase activity and 3H-cAMP binding sites in rat hippocampus during maturation and aging. Neuroscience Letters. 2001; 315:89–92. [PubMed: 11711222]

Kholwadwala D, Donnelly DF. Maturation of carotid chemoreceptor sensitivity to hypoxia: in vitro studies in the newborn rat. Journal of Physiology. 1992; 453:461–473. [PubMed: 1464840]

Kim I, Yang DJ, Donnelly DF, Carroll JL. Fluoresceinated peanut agglutinin (PNA) is a marker for live O(2) sensing glomus cells in rat carotid body. Advances in Experimental Medicine and Biology. 2009; 648:185–190. [PubMed: 19536480]

Kumar P, Prabhakar NR. Peripheral chemoreceptors: function and plasticity of the carotid body. Comprehensive Physiology. 2012; 2012:141–219. http://dx.doi.org/10.1002/cphy.c100069. [PubMed: 23728973]

Lahiri S, Roy A, Baby SM, Hoshi T, Semenza GL, Prabhakar NR. Oxygen sensing in the body. Progress in Biophysics and Molecular Biology. 2006; 91:249–286. [PubMed: 16137743]

Lahiri S, Forster RE. CO_2/H(+) sensing: peripheral and central chemoreception. International Journal of Biochemistry and Cell Biology. 2003; 35:1413–1435. [PubMed: 12818238]

Lahiri S, Iturriaga R, Mokashi A, Botré F, Chugh D, Osanai S. Adaptation to hypercapnia vs intracellular pH in cat carotid body: responses in vitro. Journal of Applied Physiology. 1996; 80:1090–1099. [PubMed: 8926231]

Nunes AR, Monteiro EC, Johnson SM, Gauda EB. Bicarbonate-regulated soluble adenylyl cyclase (sAC) mRNA expression and activity in peripheral chemoreceptors. Advances in Experimental Medicine and Biology. 2009; 648:235–241. http://dx.doi.org/10.1007/978-90-481-2259-2_27. [PubMed: 19536486]

Pastor-Soler N, Beaulieu V, Litvin TN, Da Silva N, Chen Y, Brown D, Buck J, Levin LR, Breton S. Bicarbonate-regulated adenylyl cyclase (sAC) is a sensor that regulates pH-dependent V-ATPase recycling. Journal of Biological Chemistry. 2003; 278:49523–49529. [PubMed: 14512417]

Peréz-García MT, Almaraz L, González C. Effects of different types of stimulation on cyclic AMP content in the rabbit carotid body: functional significance. Journal of Neurochemistry. 1990; 55:1287–1293. [PubMed: 1697891]

Pepper DR, Landauer RC, Kumar P. Postnatal development of CO_2 –O_2 interaction in the rat carotid body in vitro. Journal of Physiology. 1995; 485:531–541. [PubMed: 7666372]

Ramos LS, Zippin JH, Kamenetsky M, Buck J, Levin LR. Glucose and GLP-1 stimulate cAMP production via distinct adenylyl cyclases in INS-1E insulinoma cells. Journal of General Physiology. 2008; 132:329–338.10.1085/jgp.200810044 [PubMed: 18695009]

Ridderstråle Y, Hanson MA. Histochemical localization of carbonic anhydrase in the cat carotid body. Annals of the New York Academy of Sciences. 1984; 429:398–400. [PubMed: 6204572]

Rigual R, Lopez-Lopez JR, Gonzalez C. Release of dopamine and chemoreceptor discharge induced by low pH and high PCO_2 stimulation of the cat carotid body. Journal of Physiology. 1991; 433:519–531. [PubMed: 1841956]

Rocher A, Caceres AL, Almaraz L, Gonzalez C. EPAC signalling pathways are involved in low PO_2 chemoreception in carotid body chemoreceptor cells. Journal of Physiology. 2009; 587:4015–4027. [PubMed: 19581380]

Rocher A, Obeso A, Gonzalez C, Herreros B. Ionic mechanisms for the transduction of acidic stimuli in rabbit carotid body glomus cells. Journal of Physiology. 1991; 433:533–548. [PubMed: 1668755]

Sadana R, Dessauer CW. Physiological roles for G protein-regulated adenylyl cyclase isoforms: insights from knockout and overexpression studies. Neurosignals. 2009; 17:5–22. [PubMed: 18948702]

Schmid A, Sutto Z, Nlend MC, Horvath G, Schmid N, Buck J, Levin LR, Conner GE, Fregien N, Salathe M. Soluble adenylyl cyclase is localized to cilia and contributes to ciliary beat frequency regulation via production of cAMP. Journal of General Physiology. 2007; 130:99–109. [PubMed: 17591988]

Summers BA, Overholt JL, Prabhakar NR. CO(2) and pH independently modulate L-type Ca(2+) current in rabbit carotid body glomus cells. Journal of Neurophysiology. 2002; 88:604–612. [PubMed: 12163513]

Sun XC, Cui M, Bonanno JA. [HCO_3^-]-regulated expression and activity of soluble adenylyl cyclase in corneal endothelial and Calu-3 cells. BMC Physiology. 2004; 4:8. [PubMed: 15117409]

Tan ZY, Lu Y, Whiteis CA, Benson CJ, Chapleau MW, Abboud FM. Acid-sensing ion channels contribute to transduction of extracellular acidosis in rat carotid body glomus cells. Circulation Research. 2007; 101:1009–1019. [PubMed: 17872465]

Thomas JA, Buchsbaum RM, Zimniack A, Racker A. Intracellular pH measurements in Ehrlich ascites tumor cells utilizing spectroscopic probes generated in situ. Biochemistry. 1976; 18:2210–2218. [PubMed: 36128]

Townsend PD, Holliday PM, Fenyk S, Hess KC, Gray MA, Hodgson DR, Cann MJ. Stimulation of mammalian G-protein-responsive adenylyl cyclases by carbon dioxide. Journal of Biological Chemistry. 2009; 284:784–791. [PubMed: 19008230]

Travis DM. Molecular CO_2 is inert on carotid chemoreceptor: demonstration by inhibition of carbonic anhydrase. Journal of Pharmacology and Experimental Therapeutics. 1971; 178:529–540. [PubMed: 5571902]

Wang GP, Xu CS. Reference gene selection for real-time RT-PCR in eight kinds of rat regenerating hepatic cells. Molecular Biotechnology. 2010; 46:49–57. [PubMed: 20339955]

Wilding TJ, Cheng B, Roos A. pH regulation in adult rat carotid body glomus cells. Importance of extracellular pH, sodium, and potassium. Journal of General Physiology. 1992; 100:593–608. [PubMed: 1294152]

Zhang M, Nurse CA. CO2/pH chemosensory signaling in co-cultures of rat carotid body receptors and petrosal neurons: role of ATP and Ach. Journal of Neurophysiology. 2004; 92:3433–3445. [PubMed: 15056681]

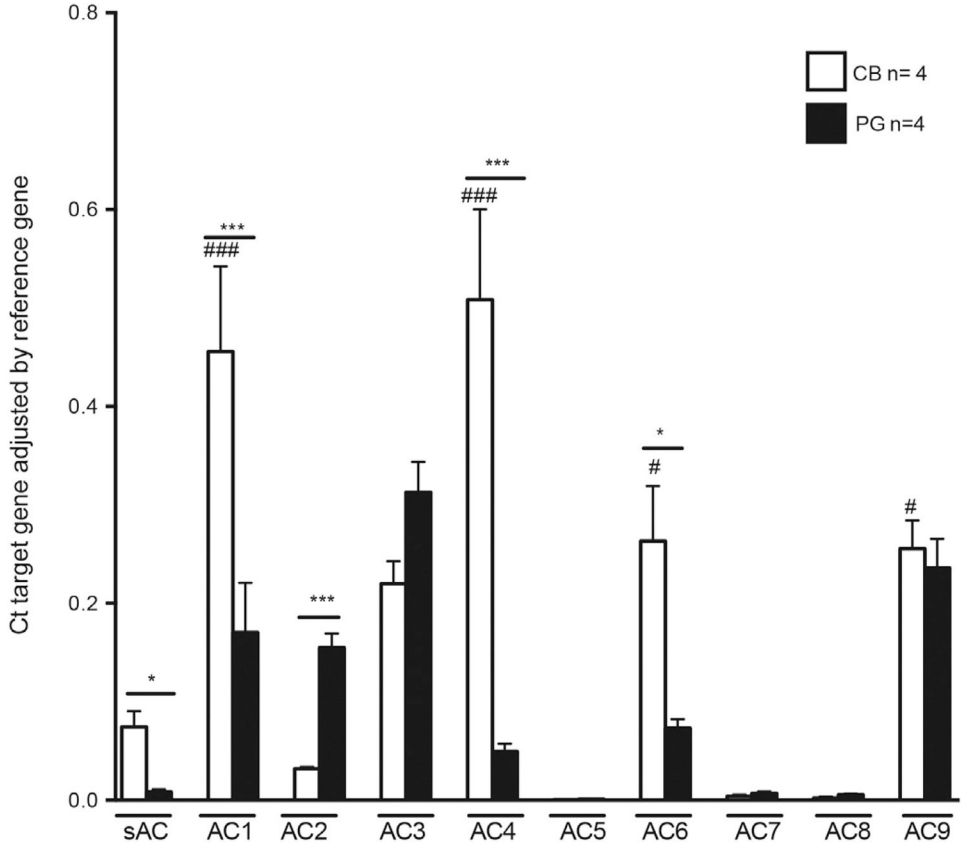

Fig. 1.

tmAC mRNA expression is higher than sAC in the carotid body (CB) and petrosal ganglia (PG). Adenylyl cyclase expression was quantified by qRT-PCR and analyzed by relative quantification to the reference gene based on the threshold cycle (C_T, $2^{\Delta C_T}$, where $\Delta C_T = C_{T,reference} - C_{T,target}$). Error bars indicate mean ± SEM. Two way repeated measurements ANOVA with Bonferroni post hoc test: $^{*}p < 0.05$ and $^{***}p < 0.001$ for comparison of the same AC isoform between different tissues (CB and PG) and $^{\#}p < 0.05$ and $^{\#\#\#}p < 0.001$ for comparison between sAC and different tmAC in the CB.

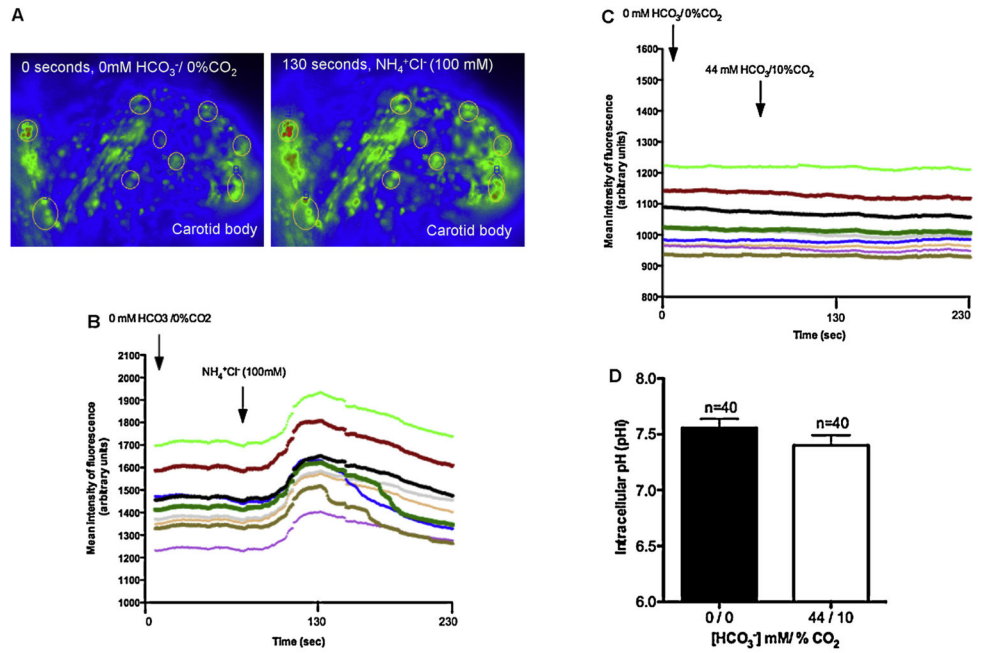

Fig. 2.

(A–D) Changes in HCO_3^-/CO_2 do not alter intracellular pH (pH_i) in the superfused carotid body. (A) Representative photomicrographs of the CB showing changes in BCECF dye fluorescent intensity (pseudocolor) in the ROI captured prior to (left panel) or in response to exposure to NH_4^+ Cl^- for 30 s (100 mM, right panel). Increased green pseudocolour and red areas in the ROI in the right photomicrograph represents increasing areas of fluorescent intensity corresponding to increased pH_i. Tracing below photomicrographs was obtained prior to, during and after exposure to NH_4^+ Cl^- (100 mM). (C) Representative tracing from one experiment showing no change in mean fluorescence intensity (pH_i) for the ROIs in the CB when the superfusate was changed from 0 mM HCO_3^-/0%CO_2 to 44 mM HCO_3^-/ 10%CO_2. (D) Composite data obtained from four different preparations, with a total of different 40 ROIs showing no change in mean fluorescence intensity. Error bars indicate mean ± SEM. A control experiment with NH_4Cl showed that there was a distinct change in fluorescent intensity CB cells (A and B). Furthermore, incremental changes in fluorescent intensity associated with changes in extracellular pH (6.5–8.0) were observed using the nigericin (10 μM)/high K^+ method to construct calibration curves. No variation in pH_i associated with changes from 0 mM HCO_3^-/0%CO_2 to 44 mM HCO_3^-/10%CO_2 within each selected region of the whole CB was observed (C and D), confirming that pH_i is maintained in isohydric hypercapnia.

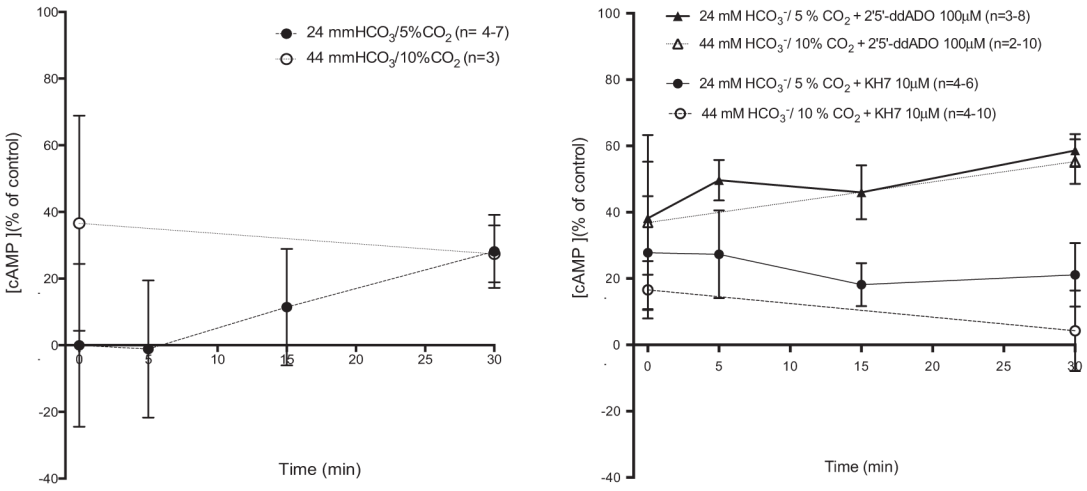

Fig. 3.

Effect of different concentrations of HCO_3^-/CO_2 on the levels of cAMP in the carotid body during 0–30 min of incubation in (A) the absence or (B) presence of adenylyl cyclases inhibitors. cAMP levels formed under 0 mM HCO_3^-/CO_2 during the different incubation times (0–30) were subtracted from the cAMP levels accumulated under normocapnia or isohydric hypercapnia. 0% control was obtained by normalization with 0 mM $HCO_3/0\%CO_2$ for each time point: 36.6 ± 8.9 fmol/µg protein, n = 4 at 0 min; 84.9 ± 19.5 fmol/µg protein, n = 6 at 5 min; 60.2 ± 10.8 fmol/µg protein, n = 4 at 15 min; 81.4 ± 10.2 fmol/µg protein, n = 6 at 30 min. Error bars indicate mean ± SEM.

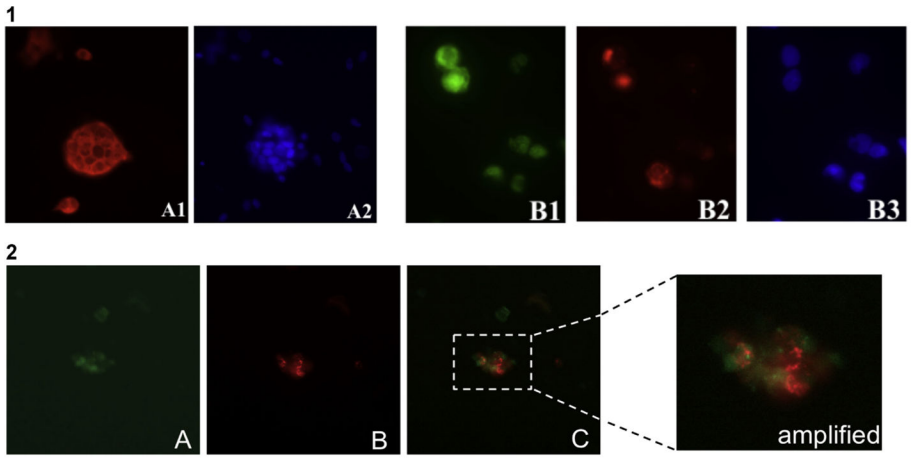

Fig. 4.

(4.1) Identification of type I cells by tyrosine hydroxylase (TH) immunostaining (A1 and A2) and identification of type I cells by fluoresceinated peanut agglutin (PNA) and TH co-staining (B1–B3). (A1) Type I cells were stained with anti-TH polyclonal rabbit antibody (1:50) and detected using rhodamine donkey anti-rabbit secondary antibody (1:100). (A2) Nuclei of type I cells was stained with DAPI. 400-fold magnification. (B1) TH staining (1:50, mouse monoclonal TH antibody visualized using FITC goat anti-mouse antibody, 1:100). (B2) PNA staining (30 μg/ml in cell culture media for 1 h visualized by TRITC filter after incubation with Rho-PNA in cell culture media during 1 h, 37 °C. (B3) DAPI staining showing more than type I cell in the CB cell culture (1000-fold magnification). (4.2) PNA-labeled type I cells expressing A-kinase activity reporter (AKAR3). (A) AKAR3 expression visualized with the FICT channel. (B) Type I cells labeled with Rho-PNA visualized with TRITC channel. (C) Co-localization of AKAR3 and Rho-PNA, confirming the infection of type I cells with AKAR3. 400-fold magnification.

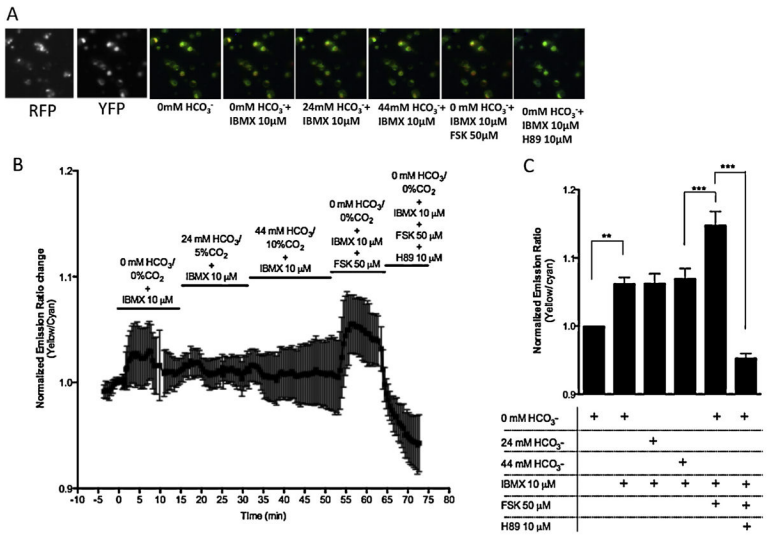

Fig. 5.

Forskolin (FSK) but not change in HCO_3^-/CO_2, increases PKA activity in type I cells of the carotid body. Effect of activators of sAC and tmAC on PKA activity in type I cells using FRET-based reporters. (A) RFP image showing PNA labeling in type I cells, YFP image showing the expression of the 3rd generation of A-Kinase activity reporter (AKAR3) and pseudocolor images showing the response of AKAR3 to different concentrations of HCO_3^-/CO_2 (0/0–44/10), forskolin (FSK, 50 μM, tmAC activator) and H89 (10 μM, PKA inhibitor) in the presence of IBMX (10 μM, non-selective PDE inhibitor), 40×. (B) Time course of representative response to HCO_3^-/CO_2 (0/0–44/10 mM/%), FSK (50 μM) and H89 (10 μM) in the presence of IBMX (10 μM, $n = 14$ cells). (C) Composite data showing that emission ratio increased by 1.6 ± 4.8% with addition of IBMX, did not significantly change with the addition of 24 or 44 mM HCO_3^-, markedly increased to 7.4 ± 1.1% with addition of FSK and decreased 14.6 ± 1.4% with H89 ($n = 21$ cells). Paired *t*-test $^{**}p < 0.01$ and $^{***}p < 0.001$. Error bars indicate mean ± SEM.

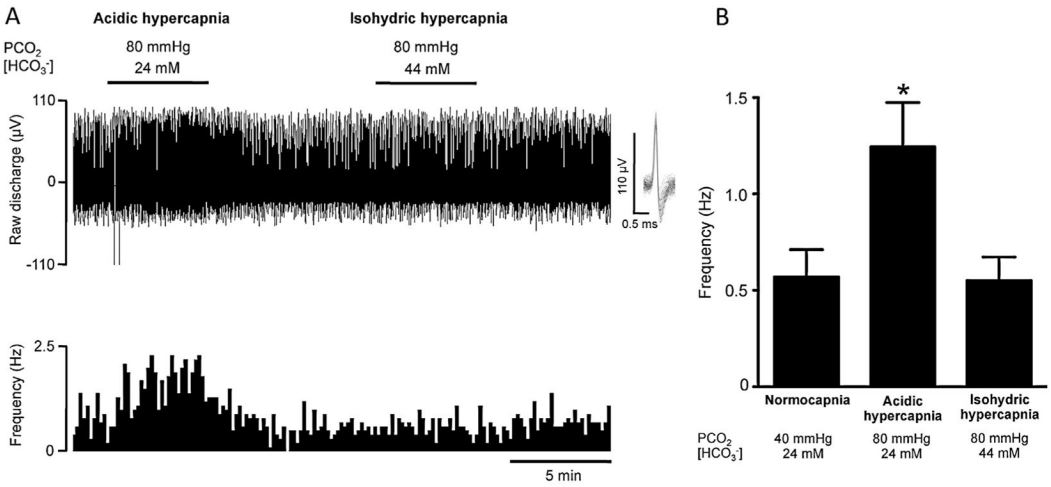

Fig. 6.

Acidic hypercapnia but not isohydric hypercapnia induces chemoafferent stimulation. (A) An example extracellular recording showing raw chemoafferent discharge (upper) and frequency interval histograms in 10 s groups (lower), recorded in control normocapnia, acidic hypercapnia and isohydric hypercapnia. Overdrawn action potentials are shown inset to demonstrate the single fiber discrimination used to obtain the frequency histograms. (B) Mean frequencies measured in normocapnia, acidic hypercapnia and isohydric hypercapnia. A significant elevation in single fiber discharge frequency was observed in acidic but not isohydric hypercapnia. Error bars indicate mean ± SEM. * denotes $p < 0.05$ compared with normocapnic frequency; one way repeated measures ANOVA with Dunnett's post hoc analysis.

Table 1

Sequence of the primers used for sAC, tmAC and reference genes.

Gene name	Direction	Primer sequence (5′–3′)	Product size (bp)
sAC[a]	Sense Antisense	CATGAGTAAGGAATGGTGGTACTCA AGGGTTACGTTGCCTGATACAATT	111
AC1[b]	Sense Antisense	ACCAGCCAAGAGGATGAAGTT ATACCAGCAGCAGCAGGACAG	446
AC2[b]	Sense Antisense	GGGAAGATTAGTACCACGGAT AGGAGAAGCCAAGGATGGACG	334
AC3[b]	Sense Antisense	ATGAGCACGAACTGAACCAGCT GTCCCATGTAGTACTGGAGACAGCTC	456
AC4[b]	Sense Antisense	AGCCAGCCTACCCAGGTT GCTTGGGTCTGAGGTCA	283
AC5[b]	Sense Antisense	CAGAGAACCAACTCCATTGGACACAATCCG CACACAGGCGTAGATCACAGATATTTTCAC	456
AC6[b]	Sense Antisense	TGCTGCTGGTCACCGTGCTCAT GGACGCTAAGCAGTAGATCATAGTTGTCAA	495
AC7[b]	Sense Antisense	GCTCCTACTGAAGCCCAAGTTC AATCACTCCAGCAATCACAGGC	256
AC8[b]	Sense Antisense	CAGTCTGGGCCTGAGGAAATT AAGTCAGGTTCTTCAAGGGTA	478
AC9[b]	Sense Antisense	ACCTACCTTTACCCAAAGTGCACGGACAAT CTCGGCGCTGCCTCACACACTCTTTGAGAC	360
G6PDH	Sense Antisense	GAAGCCTGGCGTATCTTCAC GTGAGGGTTCACCCACTTGT	162
GAPDH[c]	Sense Antisense	CACGGCAAGTTCAACGGCACAGTCA GTGAAGACGCCAGTAGACTCCACGAC	152
β-Actin	Sense Antisense	GGCCAACCGTGAAAAGATGACC GCCACGCTCGGTCAGGATCTTC	253

[a] Pastor-Soler et al. (2003).

[b] Chang et al. (2003).

[c] Wang and Xu (2010).